Int. j. adv. multidisc. res. stud. 2026; 6(2):1496-1499

Received: 26-02-2026
Accepted: 06-04-2026

International Journal of Advanced Multidisciplinary Research and Studies

ISSN: 2583-049X

Effectiveness of a Resonantly Designed Horn - Workpiece System Design in Ultrasonic Vibration - Assisted Milling

Pham Thanh Cuong
Thai Nguyen University of Technology, Viet Nam

Corresponding Author: **Pham Thanh Cuong**

Abstract
Hard milling of tool steel commonly encounters substantial difficulty in simultaneously achieving a high material removal rate (MRR) and low surface roughness (R_a). In ultrasonic vibration-assisted milling (UVAM), the vibration amplitude A is a highly influential process parameter; however, this amplitude can only be generated when the ultrasonic excitation and transmission system is correctly designed to operate under resonant conditions and remains stable under cutting load. This paper clarifies the relationship between the calculation and design of a resonant ultrasonic horn-workpiece system at 20 kHz and the resulting improvement in material removal rate and surface roughness in UVAM. The results indicate that the calculation and resonant design of the horn-workpiece ultrasonic vibration system at 20 kHz constitute the key enabling factor for the significant enhancement of MRR and R_a. By measuring the vibration amplitude (A) at the end face of the workpiece and calibrating the relationship between vibration amplitude A and workpiece length L_p to reproducibly restore the target vibration amplitude A, a four-factor Box-Behnken experimental design involving A, V_c, V_f, and a_e was established. Experimental trials were then carried out for both ultrasonic vibration-assisted milling and conventional milling. The results show that ultrasonic vibration-assisted milling significantly increases the material removal rate while markedly reducing surface roughness compared with conventional milling.

Keywords: Ultrasonic Vibration-Assisted Milling, Ultrasonic Horn, Resonant Vibration, Calibration, A-L_p Relationship, Box-Behnken Design

1. Introduction

Ultrasonic vibration-assisted milling (UVAM) is a branch of vibration-assisted machining in which low-amplitude ultrasonic oscillations are superimposed on either the tool or the workpiece in order to improve the cutting state [1-3]. Recent review studies on UVAM have highlighted its growing role in enhancing the machining performance of difficult-to-cut materials, while also emphasizing the necessity of properly designing the generator-transducer-horn system to ensure resonance tracking and efficient vibration transmission under dynamic loading conditions [4].

In many UVAM optimization studies, the vibration amplitude A has been treated as a directly controllable process variable [5-14]. However, from an experimental standpoint, the vibration amplitude A does not depend solely on ultrasonic power; it is also governed by horn design, loading configuration, assembly conditions, and the resonance-tracking state of the ultrasonic system [3, 15-18]. Without proper calibration and measurement, the vibration amplitude A may drift, thereby undermining the reliability of the optimization results. This paper presents the relationship between the calculation and design of a resonant ultrasonic horn-workpiece system operating at 20 kHz and its effectiveness in improving the material removal rate and surface roughness in UVAM. This relationship is investigated by incorporating the resonant horn-workpiece ultrasonic system into the optimization workflow, specifically by using a 20 kHz horn-workpiece resonant system to generate stable one-dimensional ultrasonic vibration along the axial Z direction, with the ultrasonic vibration applied directly to the workpiece; calibrating the vibration amplitude A as a function of the workpiece length L_p; and then employing the vibration amplitude A as a decision variable in the Box-Behnken experimental design [19]. Therefore, the significant improvements in MRR and R_a are interpreted as the direct consequence of reliably activating ultrasonic vibration at 20 kHz through an optimally designed horn-workpiece system.

The horn-workpiece ultrasonic vibration system was established using 90CrSi steel. The basic design parameters were as

follows: density ρ = 7706 kg/m³, Young's modulus E = 205 GPa, design frequency f = 20 kHz, acoustic wave velocity C = 5157.78 m/s, and a total horn-workpiece system length equal to half a wavelength, L = λ/2 = 128.94 mm. The horn, with length L_1, was designed as shown in Figure 1a and fabricated as shown in Figure 1b.

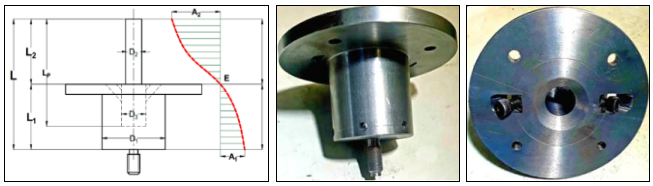

(a) (b)

Fig 1: Fabricated ultrasonic horn with a quarter-wavelength length (λ/4)

In the calculation of amplitude amplification for the stepped cylindrical horn, the input and output diameter pair, D_1 = 65 mm and D_2 = 16.5 mm, was used to determine the amplification ratio. Resonance stability was verified through impedance scanning and frequency measurement, confirming that the system operated stably at resonance at 20 kHz [20].

To enable the vibration amplitude A to be treated as a controllable variable in the design of experiments (DOE), the study performed a calibration of vibration amplitude A with respect to workpiece length L_p. As L_p was varied, the loading configuration of the horn-workpiece system changed accordingly, allowing three target amplitude levels to be achieved. The workpieces were designed as shown in Figure 2.

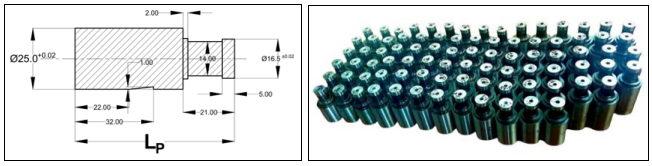

Fig 2: Workpieces

Vibration amplitude is measured at the end face of the workpieces using a Fiber Optic Displacement Sensor (Philtec, model D170, USA), a NI USB-6421 data acquisition device with a sampling rate of 250 kS/s (Hungary), and NI SignalExpress 2015 software. The analysis resolution provided by the software reached 1 µm and 1 µs, as illustrated in Figure 3.

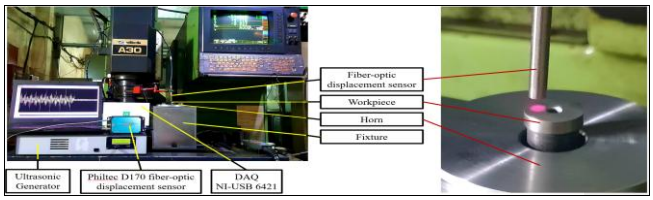

Fig 3: Experimental setup for ultrasonic vibration amplitude measurement

The calibration results showed that, within the workpiece length range of L_p = 110-120 mm, the maximum vibration amplitude reached approximately 24.8 µm. In contrast, within the workpiece length range of L_p = 56-70 mm, three target amplitude levels of A = 4, 6, and 8 µm could be generated. Specifically, workpiece lengths of L_p = 58, 62, and 66 mm corresponded to vibration amplitudes of A = 4, 6, and 8 µm, respectively. Therefore, in the optimization model, although A (µm) was treated as the input variable, L_p was regarded as the physical realization variable used to achieve the target vibration amplitude under fixed ultrasonic frequency and power conditions. Accordingly, L_p was fixed at the corresponding value for each amplitude level in the DOE, while the experimentally measured vibration amplitude A was taken as the preferred value for regression analysis.

2. Experimental Design

A Box-Behnken design (BBD) was employed with four input variables: vibration amplitude A (4, 6, 8 µm), cutting speed V_c (100, 125, 150 m/min), feed rate V_f (1062, 1327, 1592 mm/min), and radial depth of cut a_e (0.10, 0.15, 0.20 mm), each defined at three levels, as presented in Table 1.

Table 1: Input parameters of the experiments

Factor	Symbol	Unit	Level -1	Level 0	Level +1
Amplitude	A	µm	4	6	8
Cut speed	V_c	m/min	100	125	150
Feed rate	V_f	mm/min	1062	1327	1592
Radial depth of cut	a_e	mm	0.1	0.15	0.2

3. Experimental Procedure

The experimental setup and procedure are illustrated in Figure 4a. The workpieces were fabricated from hardened 90CrSi steel with a hardness of 57-58 HRC, as shown in Figure 4b. The cutting tool was a solid carbide end mill with six flutes and a diameter of 9 mm, as presented in Figure 4c. For each experimental run, the output responses, including material removal rate (MRR) and surface roughness (Ra), were recorded for both UVAM and conventional milling. In the UVAM condition, one-dimensional ultrasonic vibration at 20 kHz was directly applied to the workpiece under an ultrasonic power level of 60%. In the conventional milling condition, no ultrasonic vibration was applied. Each reported value in the table represents the average of three measurements. The experimental results are presented in Table 2.

(a) (b) (c)

Fig 4: Experimental system, workpiece, and solid carbide end mill

Table 2: Experimental results of UVAM

No	Input				Output			
	A (µm)	V_c (m/min)	V_f (mm/min)	a_e (mm)	UVAM 20kHz		CM	
					MRR (g/min)	R_a (µm)	MRR (g/min)	R_a (µm)
1	4	125	1327	0.10	3.10	0.384	2.15	0.560
2	8	125	1327	0.10	3.10	0.395	2.39	0.586
3	8	125	1592	0.15	5.39	0.436	4.05	0.680
4	6	125	1592	0.10	4.64	0.406	4.11	0.685
5	4	100	1327	0.15	4.63	0.410	3.09	0.590
6	6	125	1062	0.20	5.23	0.453	3.95	0.707
7	4	125	1062	0.15	3.69	0.437	2.76	0.671
8	6	150	1327	0.20	6.47	0.466	4.93	0.718
9	6	150	1062	0.15	4.04	0.423	3.44	0.678
10	6	125	1062	0.10	2.83	0.371	2.11	0.569
11	6	100	1327	0.10	3.27	0.398	2.64	0.627
12	6	100	1592	0.15	5.79	0.451	4.39	0.710
13	6	100	1062	0.15	3.75	0.435	2.90	0.685
14	8	125	1327	0.20	6.45	0.475	5.58	0.767
15	4	150	1327	0.15	4.83	0.365	3.32	0.529
16	6	125	1327	0.15	4.60	0.389	3.25	0.585
17	6	125	1327	0.15	4.71	0.393	3.41	0.598
18	6	125	1327	0.15	4.40	0.380	3.18	0.574
19	4	125	1327	0.20	6.60	0.473	4.23	0.679
20	8	150	1327	0.15	4.47	0.372	3.79	0.596
21	4	125	1592	0.15	5.64	0.444	3.87	0.641
22	8	100	1327	0.15	4.36	0.402	2.72	0.572
23	6	125	1592	0.20	7.39	0.485	6.59	0.873
24	6	100	1327	0.20	6.33	0.474	4.81	0.756
25	6	150	1592	0.15	5.80	0.440	4.67	0.701
26	8	125	1062	0.15	3.63	0.444	2.17	0.609
27	6	150	1327	0.10	3.34	0.381	2.52	0.597
28	6	125	1327	0.15	4.82	0.386	3.62	0.602
29	6	125	1327	0.15	4.74	0.387	3.34	0.574

4. Evaluation of the effectiveness of UVAM relative to conventional milling

Across the 29 Box-Behnken runs, UVAM yielded an MRR of approximately 2.83 - 7.39 g/min and an R_a of approximately 0.365 - 0.485 µm, whereas conventional milling produced an MRR of approximately 2.11 - 6.59 g/min and an R_a of approximately 0.529 - 0.873 µm. On a run-by-run basis, UVAM increased MRR by approximately 112% - 167% while simultaneously reducing R_a by 19 - 44% relative to conventional milling over the investigated parameter domain. This trend is consistent with the UVAM literature concerning the role of vibration-generation conditions in enhancing machining performance.

Comparative plots of material removal rate and surface roughness between ultrasonic vibration-assisted milling and conventional milling are presented in Figures 5 and 6, respectively.

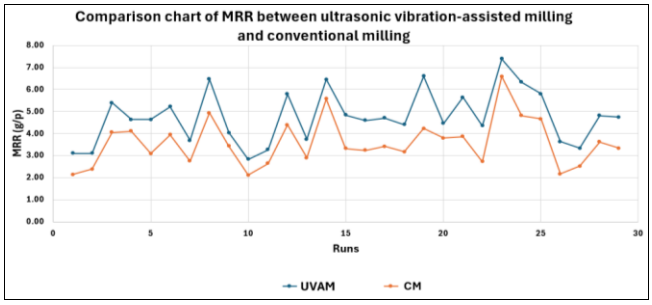

Fig 5: Comparison of material removal rate (MRR) between ultrasonic vibration-assisted milling and conventional milling

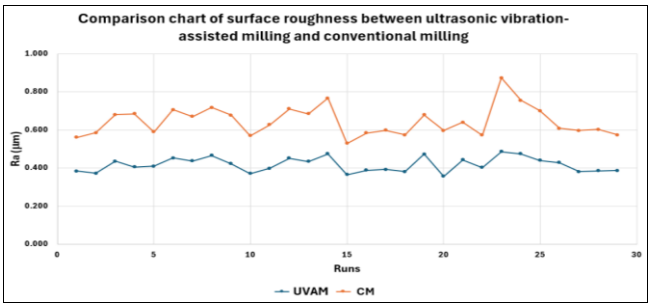

Fig 6: Comparison of surface roughness between ultrasonic vibration-assisted milling and conventional milling

5. Discussion

The present study emphasizes a necessary practical condition for meaningful UVAM optimization: the vibration amplitude A must be a measurable variable, with a clearly defined feasible range and reproducible values across experimental runs. The resonant horn-workpiece vibration system operating at 20 kHz provides precisely this condition. Specifically, the horn design determines the feasible amplitude range of A; calibration of vibration amplitude A through the workpiece length L_p converts a loading-configuration parameter into a practical control mechanism for A; and resonance verification serves as a quality-control barrier to ensure the consistency of the DOE dataset.

The comparative evaluation between UVAM and conventional milling demonstrates that UVAM offers substantial benefits in machining hardened 90CrSi steel. This improvement is attributed to the application of ultrasonic vibration at 20 kHz with an appropriate amplitude, which promotes intermittent tool-workpiece contact. Such an intermittent cutting regime is believed to reduce cutting forces and thereby significantly improve surface finish. In addition, ultrasonic vibration is associated with the acoustic softening effect, which facilitates material removal, increases the effective cutting rate, and shortens machining time, thereby leading to a marked improvement in MRR.

Flowchart of the theoretical design of the ultrasonic vibration horn-workpiece system and its experimental optimization in Figures 7.

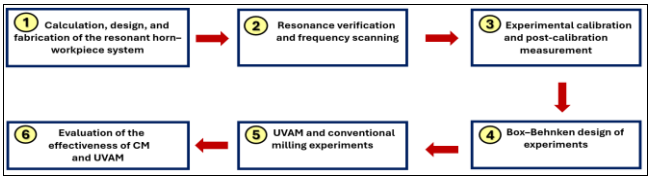

Fig 7: Flowchart of the theoretical design of the horn-workpiece system and its experimental optimization

6. Conclusions

This paper clarified the integrated relationship among the calculation, design, and experimental optimization of an ultrasonic horn for UVAM by adopting a resonantly designed horn-workpiece vibration system operating at 20 kHz and calibrating the ultrasonic vibration amplitude A as a function of workpiece length L_p, thereby enabling A to be treated as a measurable and controllable decision variable. On this basis, a Box-Behnken design was established, and a comparative experimental investigation between ultrasonic vibration-assisted milling and conventional milling was

carried out. In addition, a flowchart for the implementation of UVAM was proposed.

The results confirmed that the calculation and optimal design of the horn-workpiece vibration system, together with amplitude realization through adjustment of the workpiece length L_p, constitute the key enabling factor for improving both material removal rate and surface roughness in UVAM. This approach also makes multi-objective optimization practically feasible and provides a foundation for future studies aimed at extending the optimization framework to additional responses, such as cutting force and tool wear, or incorporating further constraints, such as resonance stability.

7. Acknowledgments

This work was supported by Thai Nguyen University of Technology (TNUT).

8. References

1. Yang Z, Zhu L, Zhang G, Ni C, Lin B. Review of ultrasonic vibration-assisted machining in advanced materials. International Journal of Machine Tools and Manufacture. 2020; 156(103594):1-34. Doi: https://doi.org/10.1016/j.ijmachtools.2020.103594
2. Zhang J, Ling L, Luo D, Deng C, Huang X, Tao G, Cao H. Cutting performance and surface quality of Ti-6Al-4V by longitudinal ultrasonic vibration-assisted high-speed dry milling with coated carbide tools. Int J Adv Manuf Technol. 2023; 126:5583-5596. Doi: https://doi.org/0.21203/rs.3.rs-2208780/v1
3. Ni C, Zhu J, Wang Y, Liu D, Wang X, Zhu L. Theoretical modeling and surface roughness prediction of microtextured surfaces in ultrasonic vibration-assisted milling. Chinese Journal of Mechanical Engineering. 2024; 37:1-21. Doi: https://doi.org/10.1186/s10033-024-01033-5
4. A. L. a, Zhang X, Chen J, Shi T, Wen L, Yu T. Review of ultrasonic vibration-assisted milling technology. Precision Engineering. 2024; 91:601-616. Doi: https://doi.org/10.1016/j.precisioneng.2024.10.021
5. Chen J, Ming W, An Q, Ch M. Mechanism and feasibility of ultrasonic-assisted milling to improve the machined surface quality of 2D Cf/SiC composites, Ceramics International. 2020; 46:15122-15136. Doi: https://doi.org/10.1016/j.ceramint.2020.03.047
6. Feng Y, *et al*. Force prediction in ultrasonic vibration-assisted milling. Machining Science and Technology. 2020; 25(2):307-330. Doi: https://doi.org/10.1080/10910344.2020.1815048
7. Feng Y, *et al*. Surface roughness prediction in ultrasonic vibration-assisted milling. Journal of Advanced Mechanical Design, Systems, and Manufacturing. 2020; 14(4):1-14. Doi: https://doi.org/10.1299/jamdsm.2020jamdsm0063
8. Gao G, Xia Z, Su T, Xiang D, Zhao B. Cutting force model of longitudinal-torsional ultrasonic-assisted milling Ti-6Al-4V based on tool flank wear. Journal of Materials Processing Technology. 2021; 291(117042):1-16. Doi: https://doi.org/10.1016/j.jmatprotec.2021.117042
9. Gao G, Fu Z, Wang Y, Pan X, Xiang D, Zhao B. Ultrasonic constitutive model and its application in ultrasonic vibration-assisted milling Ti3Al intermetallics. Chinese Journal of Aeronautics. 2022; 36(7):226-243. Doi: https://doi.org/10.1016/j.cja.2022.12.016
10. Namlu RH, Yılmaz OD, Lotfisadigh B, Kılıç SE. An experimental study on surface quality of Al6061-T6 in ultrasonic vibration-assisted milling with minimum quantity lubrication, Procedia CIRP. 2022; 108:311-316. Doi: https://doi.org/10.1016/j.procir.2022.04.071
11. Peng P, *et al*. Study on the edge defects of high volume fraction 70% SiCp/Al composites in ultrasonic-assisted milling. The International Journal of Advanced Manufacturing Technology, 2022, 1-17. DOI: https://doi.org/10.21203/rs.3.rs-782256/v1
12. Engelking L, Eissel A, Schroepfer D, Treutler K, Kannengiesser T, Wesling V. Optimisation of surface residual stresses using ultrasonic-assisted milling for wire-arc additive manufactured Ni alloy components. The International Journal of Advanced Manufacturing Technology. 2023; 126:4191-4198. Doi: https://doi.org/10.1007/s00170-023-11326-z
13. Lü Q, Yang S, Yang L, Liu E, Li G, Xiang D. Optimization milling force and surface roughness of Ti-6Al-4V based on ultrasonic-assisted milling (UAM): An experimental study. Micromachines. 2023; 14(1699):1-14. Doi: https://doi.org/10.3390/mi14091699
14. Ming W, Cai C, Ma Z, Nie P, Li C, An Q. Milling mechanism and surface roughness prediction model in ultrasonic vibration-assisted side milling of Ti-6Al-4 V. The International Journal of Advanced Manufacturing Technology. 2024; 131:2279-2293. Doi: https://doi.org/10.1007/s00170-023-11109-6
15. Namlu RH, Lotfi B, Kılıç SE. Multi-axial ultrasonic vibration-assisted machining of inconel 718 using Al2O3-CuO hybrid nanofluid MQL, Procedia CIRP. 202; 123:89-94. Doi: https://doi.org/10.1016/j.procir.2024.05.018
16. Shi Z, Chen C, Yang Z, Bao Y, Gong Y. Investigation on carbon fiber fracture mechanism of honeycomb composites in longitudinal-torsional ultrasonic-assisted milling processes, Polymer Composites. 2024; 45(3):2268-2285. Doi: https://doi.org/10.1002/pc.27918
17. Wang Z, Dong Z, Bao Y, Ran Y, Kang R. Milling characteristics and damage assessment of ultrasonic vibration-assisted end milling Cf/Sic composites. Chinese Journal of Mechanical Engineering. 2024; 37(170):1-17. Doi: https://doi.org/10.1186/s10033-024-01101-w
18. Zhang Y, Ren J, Zhou J. Effect of ultrasonic vibration-assisted milling on surface quality of carbon fiber reinforced polymer, ournal of Materials Research and Technology. 2025; 36:7373-7386. Doi: https://doi.org/10.1016/j.jmrt.2025.05.023
19. Box GEP, Behnken DW. Some New Three Level Designs for the Study of Quantitative Variables, Technometrics. 1960; 2(4):455-475. Doi: https://doi.org/10.2307/1266454
20. Huy NQ, Ha MTT, Du NV. Effects of cantilever length and diameter of the cutting tool on resonance frequency in ultrasonic assisted machining. TNU Journal of Science and Technology. 2021; 226(6):25-31. Doi: https://doi.org/10.34238/tnu-jst.4103